

# Probabilistic Spatial-Temporal Segmentation of Multiple Sclerosis Lesions

Allon Shahar and Hayit Greenspan

Department of Biomedical Engineering, Tel-Aviv University, Tel-Aviv, Israel 69978  
[hayit@eng.tau.ac.il](mailto:hayit@eng.tau.ac.il); <http://www.eng.tau.ac.il/~hayit/>

**Abstract.** In this paper we describe the application of a novel statistical video-modeling scheme to sequences of multiple sclerosis (MS) images taken over time. The analysis of the image-sequence input as a single entity, as opposed to a sequence of separate frames, is a unique feature of the proposed framework. Coherent space-time regions in a four-dimensional feature space (intensity, position (x,y), and time) and corresponding coherent segments in the video content are extracted by unsupervised clustering via Gaussian mixture modeling (GMM). The Expectation-Maximization (EM) algorithm is used to determine the parameters of the model according to the maximum likelihood principle. MS lesions are automatically detected, segmented and tracked in time by context-based classification mechanisms. Qualitative and quantitative results of the proposed methodology are shown for a sequence of 24 T2-weighted MR images, which was acquired from a relapsing-remitting MS patient over a period of approximately a year. The validation of the framework was performed by a comparison to an expert radiologist's manual delineation.

## 1 Introduction

Detection and tracking of objects in image sequences are regarded as two of the most challenging problems in the field of computer vision and image processing. A novel statistical space-time (video) modeling scheme was recently proposed [1]. We extend the scheme and apply it to the automatic detection, segmentation and tracking of lesions in MR images of the brain, in particular, multiple sclerosis lesions.

Multiple sclerosis (MS) is a neurological disease primarily affecting the central nervous system. The disease is characterized by the presence of areas of demyelination and perivascular inflammation in the brain's white matter (WM), also known as multiple sclerosis lesions (MSL). Usually, MSL can be detected visually due to their appearance as regions with increased signal intensity on T2- and PD-weighted MR images. In cases of relapsing-remitting MS, which is the most common variant of the disease (about eighty percent of the patients [2]), the signs of demyelination and inflammation appear and disappear periodically [3].

The analysis of MR images may be done qualitatively, by visually estimating the disease's progress, and/or quantitatively. The most common quantitative parameter is the burden (or load) of the disease, i.e., the overall volume of the lesions. This

parameter is indicative of the patient's current state when analyzing a specific scan, and is also of clinical importance as an indication of temporal pathological processes.

To make a quantitative analysis of the brain scans of the patient, the clinician is required to perform manual segmentation of the multiple sclerosis lesions present in those scans. Because of the vast amount of data presented by the MRI modality, manual analysis is very time-consuming. Furthermore, high inter- and intra-observer variability has been demonstrated in several studies [4]. These shortcomings were the motivation for introducing automated techniques into the process of MSL segmentation and tracking in time.

Works in the field of multiple sclerosis image processing can be categorized into two main groups. One group focuses on brain image segmentation while the second focuses on lesion tracking in time. Prominent works in the field of statistical MSL segmentation include the algorithm presented by van Leemput et al. [4], and the algorithms for automated segmentation and the identification of brain structures introduced by Warfield et al. [5] and Wei et al. [6]. The above works focused on the segmentation of an individual image frame (scan). Image intensity was used as the single feature of interest. In order to introduce spatial considerations to the segmentation scheme, an anatomical atlas was incorporated into their framework. The atlas was also used to determine required initial parameters.

The task of tracking lesions over time is closely related to the segmentation problem. Kikinis et al. [7] applied frame-by-frame modeling and segmentation as a means for handling the space-time domain. Tracking mechanisms need to be incorporated in order to find correspondences across frames in the sequence and to extract the space-time profiles of the lesions. Other research groups incorporate the temporal data into the detection stage. In Gerig et al. [8] the focus is on using the temporal change of voxel features for the identification and segmentation of MSL. No segmentation procedures were applied to individual scans. For every voxel, a feature vector was calculated based on the temporal evolution of its intensity, described by the intensity vs. time graph (the voxel's temporal profile). Rey et al. [9-10] presented two approaches to the problem of lesion tracking. In [10], lesion evolution was detected by comparing two consecutive images at a time, based on optical flow considerations. In [9] a parametric model for the intensity change of a pixel on a whole set is derived and used for candidate pixel detection. In all the works described above, a voxel-based analysis is pursued. Spatial constraints based on connectivity principles are required as a post-processing stage to extract *regions* that are suspected to be lesion regions.

The objectives of the proposed probabilistic framework include three main tasks:

1. Detection of regions pertaining to relapsing-remitting multiple sclerosis lesions (i.e., lesions that change in size over time), in a sequence of two-dimensional MR scans of the brain.
2. Delineation of these regions, or in other words, segmentation of the lesions
3. Tracking of the segmented regions through the sequence, thus producing the temporal profile of the size of each dynamic lesion (a separate size vs. time plot for each lesion).

## 2 Methodology

In this section the mathematical tools at the core of our framework are presented. The first subsection is dedicated to the assumptions and apriori knowledge that motivate the design of the framework. The utilization of a GMM for modeling the image-sequence in a chosen feature-space and for statistical segmentation is described in the second subsection.

### 2.1 Model assumptions and apriori knowledge

Multiple sclerosis lesions have several typical visual features. An example of a T2-weighted image with MSL is given in Figure 1(a) (one of the lesions is marked by a surrounding circle). The most distinct of the lesions' visual features is their relatively high intensity. In addition, lesion regions are usually convex. Lesions are known to appear in the brain WM [2]. Therefore, it can be assumed that lesions are rarely on the brain's vertical centerline (the line that goes through the corpus callosum) and that high-intensity regions connected to the brain's boundaries are not lesions [7]. The intensity, shape and location characteristics are used as apriori knowledge in the design of the proposed modeling framework.

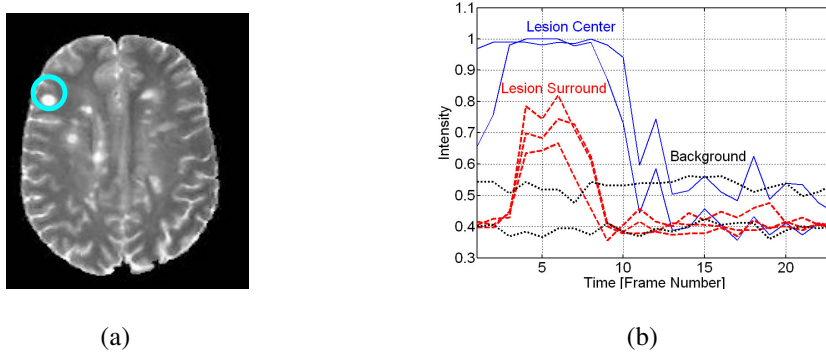


**Fig. 1.** (a) An example of a T2-weighted image of an MS patient. One of the lesions is circled. (b) Evolution in time of pixel intensity for different pixels in the encircled region in (a): lesion-center (*solid line*), lesion-surround (*dash line*), and non-lesion tissue (*dot line*).

The underlying assumption of the suggested methodology is that a Gaussian mixture model (GMM) generates the image intensities and their space-time distribution. The model is based on the following observations:

1. Gaussian behavior of the intensity feature – regarding this issue, we follow previous works that suggest modeling brain intensities by a GMM ([4-5], [7]).
2. Spatial convexity of the lesion regions.

3. Distribution of the intensity feature in time – Figure 1(b) shows the intensity vs. time plots of several pixels taken from the center of the marked lesion in Figure 1(a), from its surround and from the background. Unlike the background pixels that demonstrate noisy fluctuations around their mean intensity, the lesion pixels present a clear relapsing-remitting pattern.

Figure 1(b) teaches us of an important distinction between lesion center and lesion surround characteristics in time. While lesion-surround pixels present a pattern of behavior similar to that of the central pixels, their peak intensity is lower and the time interval in which they show a relapsing-remitting behavioral pattern is shorter. The differences may be attributed to the fact that the lesion-surround often includes a mixture of lesion and edema or lesion and normal WM ([7]). We employ this knowledge to provide a more accurate delineation of the lesion region, as will be described in the section 3.

## 2.2 GMM for image representation and segmentation

In order to construct a GMM for a given sequence of images, a transition is first made from the image domain to a selected feature-space. Following the feature extraction, each pixel is represented by a feature-vector and the image-sequence as a whole is represented by a collection of feature-vectors in the feature-space. Note that the dimensionality of the feature-vectors and the feature-space is dependent on the chosen features and may be reduced or augmented in a modular way, as needed.

Learning a Gaussian mixture model from the feature data is, in essence, an unsupervised clustering task. The EM algorithm is used to determine the GMM parameters according to the maximum likelihood principle [11]. Following the learning process, a correspondence can be made between the coherent regions in the feature space and homogeneous regions in the image plane. The probabilistic affiliation of pixel  $x$  to cluster (Gaussian)  $j$  is given by:

$$p(\text{Label}(x) = j) = \frac{\frac{\alpha_j}{\sqrt{(2\pi)^d |\Sigma_j|}} \exp\left\{-\frac{1}{2}(x - \mu_j)^T \Sigma_j^{-1} (x - \mu_j)\right\}}{\sum_{j=1}^K \frac{\alpha_j}{\sqrt{(2\pi)^d |\Sigma_j|}} \exp\left\{-\frac{1}{2}(x - \mu_j)^T \Sigma_j^{-1} (x - \mu_j)\right\}} \quad (1)$$

$K$  indicates the number of Gaussians in the learned model. The model parameters include the mean ( $\mu_j$ ), covariance matrix ( $\Sigma_j$ ) and relative weight of each Gaussian ( $\alpha_j$ ); these parameters are characterized as follows:

$$\alpha_j > 0 \quad , \quad \sum_{j=1}^k \alpha_j = 1$$

$$\mu_j \in R^d \quad , \quad \Sigma_j \text{ is a } d \times d \text{ positive definite matrix}$$

Segmentation maps are generated by assigning each pixel in the sequence to the most probable Gaussian cluster, i.e., to the component  $j$  of the model that maximizes the a posteriori probability (Equation 1).

### 3 Proposed MSL Spatial-temporal Segmentation Framework

Figure 2 presents the four-stage framework proposed (a preliminary three-stage framework was introduced in [12]). The first stage is a preprocessing stage, in which the framework's regions of interest (ROIs) are extracted (registration and bias field correction are not part of the current framework; we assume that these operations were performed on the input sequence prior to the application of our framework). In the second stage, a Gaussian mixture model (GMM) models the sequence in space-time. Space-time regions pertaining to dynamic lesions are detected, segmented and tracked in time in the third stage based on the features of the Gaussian clusters of the model. The final stage is aimed at producing a more complete delineation of the lesions via model adaptation.

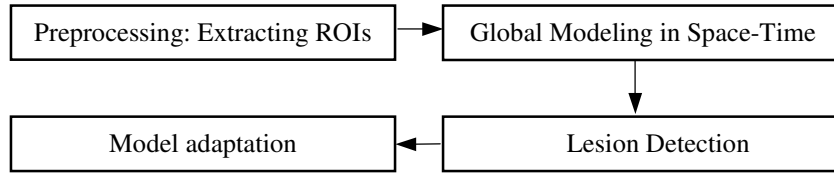


**Fig. 2.** The framework proposed for dynamic lesion detection & tracking

#### 3.1 Preprocessing: Extracting Regions of Interest

One of the most distinct visual features of MSL is their high intensity. We start by focusing on the intensity feature and model the entire sequence by an intensity-based GMM. The model parameters are determined via the EM algorithm. Initial values for the EM algorithm can be obtained by incorporating a priori knowledge (e.g., via an anatomical atlas) or by extracting the values from the data itself, as performed in our framework by employing the K-Means algorithm. The model order,  $K$ , is usually chosen within the range of 3-6, so as to reflect the number of different tissues present.  $K$  can be determined by an optimization criterion, such as the Minimum Description Length (MDL) [13].

Each component of the model represents coherent intensity clusters in the feature domain. Following the model generation, a correspondence is made between the coherent regions in the feature space and homogeneous regions in the image plane. Each pixel of each frame is assigned to the most probable Gaussian cluster, i.e. to the component of the model that maximizes the a-posteriori probability (Equation 1).

Our goal in this stage is to extract the high-intensity clusters that correspond to the high-intensity regions in the sequence. We define these regions as our regions of interest (ROIs), since they include the pixels that pertain to MS lesions. The segmented regions that correspond to the two highest-mean-intensity Gaussians clusters are extracted and are used as the input data for the following stages. We choose to extract two clusters and not just one in order to ensure that pixels pertaining to lesion-surround (typically of lower intensity, as shown in section 2.1) are included in the ROIs. In order to eliminate potential false positives (mainly pixels of a skull-CSF Partial Volume Effect) a region growing procedure removes hyper-intense regions on the boundaries of the brain.

### **3.2 Modeling and Segmenting the Sequence in the Space-Time Domain**

A global space-time model is generated next. The ROIs are modeled in a four-dimensional feature space: intensity, spatial position (x,y) and time expressed by the frame's index within the sequence. In the global model, each Gaussian corresponds to what we call a "space-time blob" [14]. The learning process of the model provides us with the parameters that characterize each blob of the model. The blob characteristics of each tracked region are stored for the lesion identification stage that follows.

Attention should be given to the fact that in the proposed methodology, a unique set of blobs is used for modeling the entire frame-sequence. The same blobs are also used in the segmentation of the sequence, as each pixel in the sequence is probabilistically affiliated to one of the blobs in the set. Connecting all the pixels in a specific frame, which were labeled as pertaining to a certain blob, yields a segmented region. Moreover, because a space-time model is used and the sequence is processed as a single entity, a certain region is marked by the same label in all the frames in which it is present. A by-product of the segmentation process is, therefore, the *temporal tracking* of regions, since their region of support is known from the segmentation maps in each frame. The unification of segmentation and tracking in our scheme is unique when compared to other works in the field [7-10].

### **3.3 Lesion Detection**

Criteria for the identification of blobs pertaining to lesions are applied to the *parameters* of the GMM. While current schemes detect lesion-voxels based on voxel-level rules (e.g., [8-10]), in this work we propose a unique set of criteria that incorporate region-based (blob) features. Such features are attainable in a direct manner from our global model, as each blob in the model corresponds to a space-time region in the sequence. Therefore, the parameters of a blob represent the intensity and space-time features of its corresponding region. Furthermore, the segmentation maps enable the incorporation of region-level features, such as the segmented region's size-profile along the sequence.

Based on context-specific knowledge, two criteria for the identification of blobs pertaining to MSL (lesion-blobs) are applied:

1. A constraint on the mean intensity of the blob; MSL appear hyper-intense in T2-weighted MR images.
2. A constraint on the blob's size variability in time; dynamic changes in the size is characteristic of MSL, since the structures of normal tissue remains relatively constant during the time period that is typical to our case.

### **3.4 Model Adaptation**

Lesion-center and lesion-surround regions have different characteristics (section 2.1). In an unsupervised modeling scheme, the entire region of the lesion is likely to be assigned to more than one blob. In order to produce a more accurate delineation of the lesion region, we suggest a merging process to combine the lesion-center pixels with those of the lesion-surround. In this stage it is assumed that all the lesion-center blobs were accurately detected in the lesion-detection stage (section 3.3). The merging procedure requires identification of lesion-surround blobs. For each lesion-center blob, a lesion-surround blob is detected according to the following criteria:

1. Mean spatial features  $(x,y)$  close, in terms of Euclidean distance, to the mean spatial features of the lesion-center. This criterion ensures the merging of spatially close regions.
2. Mean-intensity above a certain threshold, which ensures that no regions pertaining to background-blobs, erroneously included in the ROIs, are merged.
3. Temporal overlap with the lesion-center blob. This criterion ensures that in a case of two lesions appearing in the same place, but at different time-points, lesion-surround blobs are affiliated only with their corresponding lesion-center blob. Blobs that are sequential in their temporal extent, i.e. there is an interval of one frame between the disappearance of one blob and the appearance of the other are also considered as temporally overlapping.

Following the extraction of lesion-center and lesion-surround blob pairs, the segmented regions corresponding to these blobs are merged to produce an updated lesion region.

## 4 Experiments and Results

The framework was applied to a T2-weighted serial data set received from Harvard Medical School and Brigham and Women's Hospital in Boston [8]. In our experiment, a single slice from each set of 54 scans was considered. Each slice is 3-mm thick and holds a  $256 \times 256$  resolution, thus resulting in voxel dimensions of  $0.48 \times 0.48 \times 3$  mm<sup>3</sup>. The time series includes 24 frames acquired over a period of approximately a year. The data sequence underwent several preprocessing procedures [6], including sequence registration with respect to the first frame of the series, extraction of the intracranial cavity and the correction of intensity inhomogeneities.

In Figure 3 the results of the detection and merging stages are presented for four example frames (Figure 3(a)). In the preprocessing stage an intensity-based model with five components was learned. The high intensity clusters that were extracted from the sequence in this stage represent an estimation of the lesion burden present in the input. In Figure 3(b) these ROIs are darkened (this figure corresponds to the results following the removal of potential false positives). It can be noticed that all the lesions that are clearly visible in Figure 3(a) were marked, i.e., the results hold no false negatives. The regions in Figure 3(b) correspond to both static and dynamic lesions and cover the MS presence in the example frames. In Fig. 3(c) and 3(d) *only* regions that correspond to lesion-blobs that were detected as pertaining to *dynamic MSL* are color marked and labeled.

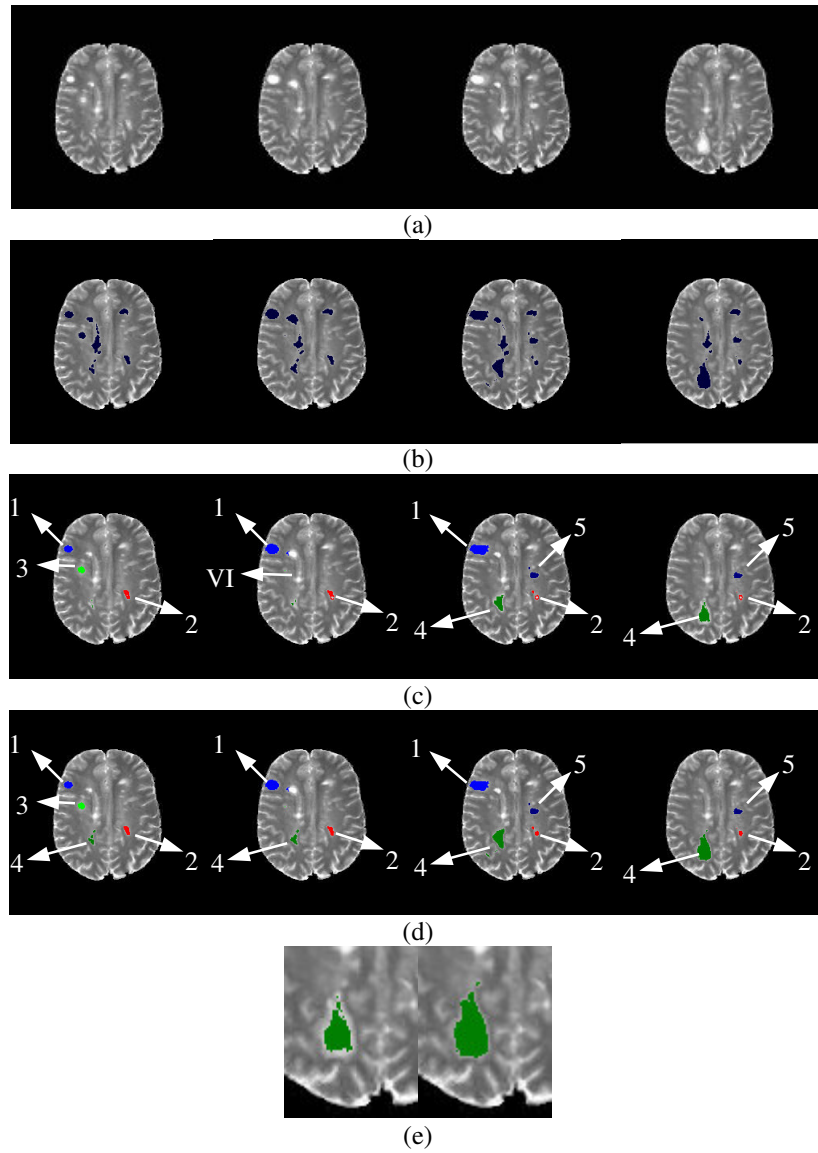
Following the preprocessing stage a space-time global GMM was constructed. The model order,  $K$ , was empirically chosen to be 75. In Figure 3(c) the results of the detection scheme are presented for the example frames. Six of the 75 extracted blobs were identified as potential lesion-blobs (five of which are shown in these frames). Each lesion-blob, which was detected by the dynamic lesions detection scheme, is marked by a different color and labeled.

Figure 3(c) demonstrates the ability of our framework to unite segmentation and tracking in time. While lesions, which show a significant size change, are all marked in at least one frame, static lesions (e.g., the one labeled 'VI') are rightfully undetected and unmarked. Even though there are no false positives in the results, lesions were not identified in some of the frames. Furthermore, the delineations of the lesions do not seem accurate as the identified blobs failed to cover the full extent of the lesion (note lesion 4).

Results at the output of the model adaptation process are shown in Figure 3(d), using the same pseudo-colors and number labels as in Figure 3(c). The set of criteria applied to each blob in the results of Figure 3(c), in order to determine if it is a lesion-surround blob, includes: (1) A distance of less than 4 pixels between the blob center and the center of a detected lesion blob; (2) Mean intensity higher than 0.6; (3) Temporal overlap with the closest (criterion 1) center-lesion blob.

The more accurate segmentation of lesions achieved by the model adaptation process is clear. A distinct improvement can be seen in Figure 3(e), which shows lesion 4 before and after the merging (image corresponds to frame 20). Overall, the

results demonstrate that the proposed scheme is effective in confronting the task of tracking highly dynamic MS lesions.



**Fig. 3.** Detection and merging results. (a) Frames [1 3 8 20] of the original sequence. (b) ROI extraction. Potential lesion-regions that were extracted in preprocessing are marked in dark color. (c) Spatial-temporal segmentation of the *dynamic* lesions. Detected regions are color marked and labeled. Static lesions are not colored. (d) Model adaptation via region merging. (e) Zoom on lesion 4 in frame 20, before (left) and after (right) model adaptation.

Figure 4 presents a plot of lesion area (in pixels) versus time for the lesions numbered 1 (triangular labeling) and 4 (circular labeling) in Figure 3. We observe a temporal evolution characteristic of relapsing-remitting MS lesions. The size estimation for these two lesions in the first ten frames of the sequence is given in Table 1.

Assessing the automated segmentation (and tracking) accuracy is problematic in the absence of a “ground truth”. We validated our results by comparing them to the output of an expert’s manual segmentation. All six dynamic lesions marked by the expert were detected by our framework. The expert’s estimation of the size evolution of lesions 1 and 4 is given in Figure 4 alongside the framework’s results and in Table 1. Although the expert typically marks larger areas, the two plots show the same pattern of disease progress, and are, therefore, clinically compatible.

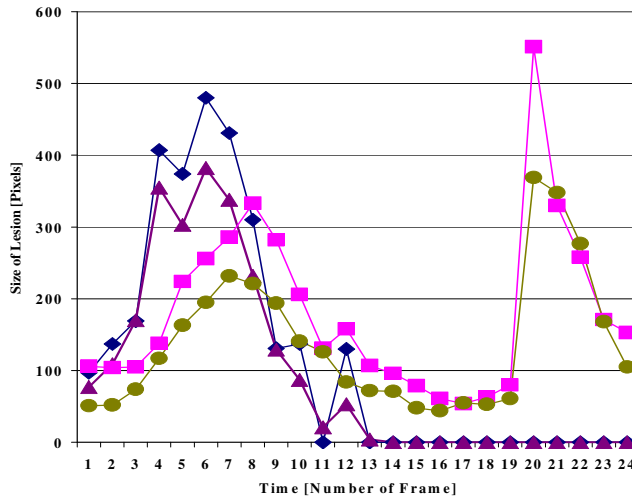


**Fig. 4.** Quantitative results and validation. The evolution in time of the size of lesions numbered 1 and 4 in Figure 3 is shown (triangular/circular labels). Results are compared to an expert’s manual delineation of the same lesions (diamond /rectangular labels).

**Table 1.** Quantitative results and validation. The size estimation of lesions numbered 1 and 4 in Figure 3 is presented for the first ten frames of the sequence. The size is calculated in number of pixels and refers to the given resolution. The framework’s results (the FW rows) are compared to an expert’s manual delineation.

| Les. |      | 1   | 2   | 3   | 4   | 5   | 6   | 7   | 8   | 9   | 10  |
|------|------|-----|-----|-----|-----|-----|-----|-----|-----|-----|-----|
| 1    | Exp. | 97  | 137 | 169 | 407 | 374 | 480 | 431 | 310 | 131 | 137 |
|      | FW   | 77  | 109 | 170 | 355 | 303 | 394 | 338 | 232 | 129 | 87  |
| 4    | Exp. | 106 | 104 | 105 | 138 | 224 | 256 | 286 | 333 | 282 | 206 |
|      | FW   | 51  | 52  | 74  | 117 | 163 | 195 | 232 | 221 | 194 | 141 |

## 4 Conclusions

In the presented study, the space-time content of an MR brain image-sequence is described using a statistical parametric methodology. We chose to model the sequence in this work by using a four-dimensional feature space (intensity, spatial position and time). While current schemes detect lesion-voxels based on voxel-level rules, in this work we propose a unique set of criteria that incorporate region-based (blob) features. Region-based features, such as the size-profile, are attainable in a direct manner from our global model, since each blob in the model corresponds to a space-time region in the sequence. This region-level analysis can be regarded as compatible to the definition of a lesion as a spatially connected entity with a unique space-time profile. Following the detection, segmentation and tracking of lesions are performed simultaneously in a unified stage of spatio-temporal segmentation, and not separately as in other works. Adding a model adaptation stage improves the framework's results, as it enables the detection of lesions at extreme points of their temporal existence and suspected edema regions around lesions.

Model initialization is critical for the capability to produce a representation of image-sequence regions that delineates accurately regions of interest and distinguishes between static and dynamic regions. The most crucial element in the initialization process is the determination of the number of blobs. In the case of a global model,  $K$  needs to be chosen as the number of expected homogeneous space-time regions in the sequence. However, this number may be large and its range unpredictable, and, therefore, it is impractical to use such criteria as the MDL to establish the model's order. We confronted the problem by suggesting a scheme that includes context-based masking as a preprocessing step, followed by an empirical choice of  $K$ . The initial masking provides a reduced region of interest for the image modeling stage, and, as a result, blobs are more likely to fit and accurately model lesion regions.

Overall, the results and their validation by comparison to manual estimation demonstrate that the proposed scheme is effective in confronting the task of tracking dynamic MS lesions. In future work, we plan to investigate larger datasets and expand the framework to volumetric data.

## Acknowledgements

We would like to thank Dr. Warfield of Harvard Medical School and Brigham and Women's Hospital in Boston for providing the multiple sclerosis image data and Prof. Gomori of Hadassah Medical Center in Jerusalem for manually marking the lesions in our data.

## References

1. Greenspan, H., Goldberger, J., Mayer, A.: Probabilistic Space-Time Modeling via Piecewise GMM. *IEEE Trans. Pattern Analysis and Machine Intelligence* **26:3** (Mar. 2004) 384-396
2. Grossman, R.I., McGowan, J.C.: Perspectives on multiple sclerosis. *American Journal of Neuroradiology* **19** (Aug. 1998) 1251-1265
3. Noseworthy, J.H., Lucchinetti, C., Rodriguez, M., Weinshenker, B.G.: Multiple Sclerosis. *The New England Journal of Medicine* **343:13** (2000) 938-952
4. Van Leemput, K., Maes, F., Vandermeulen, D., Colchester, A., Suetens, P.: Automated segmentation of multiple sclerosis lesions by model outlier detection. *IEEE Trans. on Medical Imaging* **20** (Aug. 2001) 677-688
5. Warfield, S., Dengler, J., Zaers, J., Guttman, C.R.G., Wells, W.M., Ettinger, G.J., Hiller, J., Kikinis, R.: Automatic Identification of Grey Matter Structures from MRI to Improve the Segmentation of White Matter Lesions. *Journal of Image Guided Surgery* **1:6** (1995) 326-338
6. Wei, X., Warfield, S.K., Zou, K.H., Wu, Y., Li, X., Guimond, A., Mugler III, J.P., Benson, R.R., Wolfson, L., Weiner, H.L., Guttman, C.R.G.: Quantitative Analysis of MRI Signal Abnormalities of Brain White Matter with High Reproducibility and Accuracy. *Journal of Magnetic Resonance Imaging* **15** (2002) 203-209
7. Kikinis, R., C.R.G. Guttman, D. Metcalf, W.M. Wells, G.J. Ettinger, H.L. Weiner, Jolesz, F.A.: Quantitative follow-up of patients with multiple sclerosis using MRI: technical aspects. *Journal of Magnetic Resonance Imaging* **9:4** (1999) 519-530
8. Gerig, G., Welti, D., Guttman, C.R.G., Colchester, A.C.F., Székely, G.: Exploring the discrimination power of the time domain for segmentation and characterization of active lesions in serial MR data. *Medical Image Analysis* **4:1** (Mar. 2000) 31-42
9. Rey, D., Stoeckel, J., Malandain, G., Ayache, N.: A Spatio-temporal Model-based Statistical Approach to Detect Evolving Multiple Sclerosis Lesions. In *IEEE Workshop on Mathematical Methods in Biomedical Image Analysis (MMBIA'01)*, Kauai, Hawaii, USA (Dec. 2001) 105-112
10. Rey, D., Subsol, G., Delingette, H., Ayache, N.: Automatic Detection and Segmentation of Evolving Processes in 3(d) Medical Images: Application to Multiple Sclerosis. *Medical Image Analysis* **6:4** (Dec. 2002) 163-179
11. Dempster, A., Laird, N., Rubin, D.: Maximum Likelihood from incomplete data via the EM algorithm. *J. of Royal Statistical Society* **39:1** (1977) 1-38
12. Greenspan, H., Mayer, A., Shahar, A.: A Probabilistic Framework for the Spatio-Temporal Segmentation of Multiple Sclerosis Lesions in MR Images of the Brain. In *Proceedings of SPIE International Symposium on Medical Imaging*, San Diego, USA (2003) 1551-1559
13. Cover, T.M., Thomas, J.A.: *Elements of Information Theory*. Wiley Series in Telecommunication, John Wiley and Sons, New York (1991)
14. Carson, C., Belongie, S., Greenspan, H., Malik, J.: Blobworld: Image Segmentation Using Expectation-Maximization and Its Application to Image Querying. *IEEE Trans. on Pattern Analysis and Machine Intelligence* **24:8** (Aug. 2002) 1026-1038